Light-Fidelity (Li-Fi)

LED assisted navigation in large indoor environments

Manuela Vieira, Manuel Augusto Vieira, Paula Louro, Alessandro Fantoni
ADETC/ISEL/IPL,
R. Conselheiro Emídio Navarro, 1959-007
Lisboa, Portugal
CTS-UNINOVA
Quinta da Torre, Monte da Caparica, 2829-516,
Caparica, Portugal

e-mail: mv@isel.ipl.pt, mv@isel.pt, plouro@deetc.isel.pt, afantoni@deetc.isel.ipl.pt

Pedro Vieira
ADETC/ISEL/IPL,
R. Conselheiro Emídio Navarro, 1959-007
Lisboa, Portugal
Instituto das Telecomunicações
Instituto Superior Técnico, 1049-001,
Lisboa, Portugal
e-mail: pvieira@isel.pt

***Abstract*— In this work, a Light Emitting Diode (LED) assisted navigation system for large environments is presented. The LEDs are used both for room illumination purposes and as transmitters if modulated at high frequencies. The payload data together with the identifiers, IDs, assigned to the physical location of the transmitters are broadcast using an On-Off Keying (OOK) modulated scheme. The mobile receiver is a double p-i-n/pin SiC photodetector with light controlled filtering properties. Coded multiplexing techniques for supporting communications and navigation together on the same channel are analysed. A demonstration of fine-grained indoor localization is simulated. Different indoor layouts for the LEDs are considered. Square and hexagon mesh are tested, and a 2D localization design, demonstrated by a prototype implementation, is presented. The results showed that the LED-aided Visible Light Communication (VLC) navigation system makes possible not only to determine the position of a mobile target inside the unit cell but also in the network and concomitantly to infer the travel direction in time. Bidirectional communication was tested between the infrastructure and the mobile receiver.**

Keywords- Visible Light Communication; Indoor positioning; Square and hexagonal topologies; SiC technology; Optical sensor, Navigation system; Bidirectional communication.

I. INTRODUCTION

Light Fidelity (Li-Fi) is a technology for wireless communication between devices using light, to transmit data and position. VLC/LiFi can play a significant role by bringing redundancy to traditional RF solutions. It brings strong value-added features in terms of: complexity and cost, selectivity, quality of link, high precision positioning and security. Nevertheless, one of the limitations of LiFi existing solutions is that LiFi have been developed mainly for indoor applications [1]. With the rapid advancement of smart equipment, location based services that employ different kinds of communication and positioning technologies to localize the walker and to provide relevant services, start to develop. Although Global Positioning System (GPS) works extremely well in an open-air localization, it does not perform effectively in indoor environments, due to the disability of GPS signals to penetrate in in-building materials. Nowadays, indoor positioning methods are mainly based on Wi-Fi, Bluetooth, Radio-frequency identification (RFID), visible light communications (VLC) and inertia navigation [2, 3, 4, 5, 6]. Although many methods are available such as WiFi-based [7, 8] and visual indoor topological localization [9, 10], they require dense coverage of WiFi access points or expensive sensors, like high-performance cameras, to guarantee the localization accuracy.

VLC is a data transmission technology [11, 12, 13, 14]. VLC can easily be employed in indoor environments such as offices, homes, hospitals, airplanes/airports and conference rooms. Compared with other positioning methods, indoor VLC based positioning, has advantages, since it can use the existing LED lighting infrastructure with simple modifications. Due to the combination of illumination and communication, a lot of investigations have been attracted in VLC applications [15, 16, 17]. The system considers both positioning and lighting, thus it will save energy and realize high accuracy positioning with low cost at the same time. Besides that, due to the advantage of electromagnetic free, VLC based positioning is a green positioning method.

In the sequence, we propose to use modulated visible light, carried out by white low cost LEDs, to provide globally consistent signal-patterns and engage indoor localization. The LEDs are capable of switching to different light intensity levels at a very fast rate. The switching rate is fast enough to be imperceptible by a human eye. This functionality can be used for communication where the data is encoded in the emitting light in different ways [18]. A photodetector can receive the modulated signals and decode the data. This means that the LEDs be twofold of providing illumination as well as communication.

The requirement of managing access to multiple devices in VLC is different from other types of networks. This is because the size of a cell can vary depending on how illumination is provided. The task of squaring the circle proposed by ancient geometers was proven to be impossible. The triangle of largest area of all those inscribed in a given circle is equilateral. The cells of a beehive honeycomb are hexagonal. So, research is necessary to design LED arrangements that can optimize communication performance while meeting the illumination constraints for a variety of indoor layouts, using four-code assignment for the LEDs in an extended equilateral triangle, square or diamond mesh. The main idea is to divide the space into spatial beams originating from the different light sources, and identify each beam with a unique timed sequence of light signals. The receiver, equipped with an a-SiC:H pinpin photodiode, determines its physical position by detecting and decoding the light signals. The overlap of different light beams at the receiver is used as an advantage to increase the positioning accuracy. Fine-grained indoor localization can enable several applications; in supermarkets and shopping malls, exact location of products can greatly improve the customer's shopping experience and enable customer analytics and marketing [19, 20].

Luminaires equipped with multi colored LEDs can provide further possibilities for signal modulation and detection in VLC systems [21]. The use of Red-Green-Blue (RGB) LEDs is a promising solution as they offer the possibility of Wavelength Division Multiplexing (WDM) which can enhance the transmission data rate. A WDM receiver have been developed [22, 23]. The device is based on tandem a-SiC:H/a-Si:H pin/pin light controlled filter. When different visible signals are encoded in the same optical transmission path, the device multiplexes the different optical channels, performs different filtering processes (amplification, switching, and wavelength conversion) and finally decodes the encoded signals recovering the transmitted information.

In this paper, a LED-assisted indoor positioning and navigation VLC system, for large indoor environment is proposed. The principle of the positioning scheme and the algorithm to decode the information are described and experimental results are presented. A 2D localization design, demonstrated by a prototype implementation is tested. Fine-grained indoor localization is demonstrated using square and hexagonal topologies. Finally, conclusions are addressed. The proposed, composed data transmission and indoor positioning, involves wireless communication, smart sensoring and optical sources network, building up a transdisciplinary approach framed in cyber-physical systems.

II. SYSTEM CONFIGURATION

A VLC system consists on a VLC transmitter that modulates the light produced by LEDs and a VLC receiver based on a photosensitive element that receive and analyses the transmitted modulated signals. The transmitter and the receiver are physically separated, but connected through the VLC channel. For VLC systems, Line of Sight (LoS is a mandatory condition.

LED bulbs work as transmitters, broadcasting the information. An optical receiver extracts its location to perform positioning and, concomitantly, the transmitted data from each transmitter. Multiple LEDs can transmit simultaneously to the same receiver using joint transmission. To synchronize the signals from multiple LEDs, the transmitters use different ID´s, such that the signal is constructively at the receiver.

A. *Shapes and topologies*

Different shapes, for the unit cell, are proposed based on the joint transmission of four modulated LEDs: the square, the hexagonal. The unit cells, for the analyzed topologies, are displayed in Figure 1.

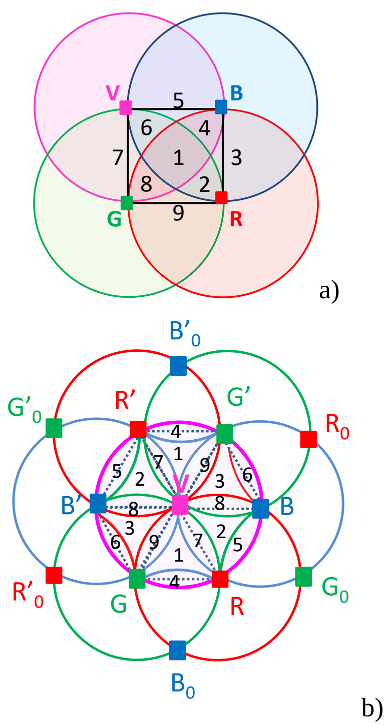

Figure 1. Top-down view of unit cells (LED array = RGBV color spots) having each one four modulated RGBV-LEDs located at the corners of the grid. a) Square cell. b) First hexagon ring.

In Figure 1a, the proposed LED arrangement employs four modulated LEDs placed at the corners of a square grid.

In Figure 1b, a cluster of three diamond cells sharing the violet node, fill the space with a hexagon, leading to the hexagonal topology. The estimated distance from the ceiling lamp to the receiver is used to generate a circle around each transmitter on which the device must be located in order to receive the transmitted information (generated location and coded data).

In all topologies, the grid sizes were chosen to avoid overlap in the receiver from adjacent grid points. To improve its practicality, the tested geometric scenario for the calculations, in both topologies, uses a grid in smaller size (2 cm between adjacent nodes). To receive the information from several transmitters, the receiver must be positioned where the circles from each transmitter overlap, producing at the receiver, a MUX signal that, after demultiplexing, acts twofold as a positioning system and a data transmitter. The generated regions, defined onwards as footprints, are pointed out in Figure 1 and reported in Table I.

TABLE I FINE-GRAINED CELL TOPOLOGY.

Footprints regions	Square topology	Hexgonal topology
P#1	RGBV	RGV R'G'V
P#2	RGB	RBV R'B'V
P#3	RG	G'BV GB'V
P#4	RBV	RGB_0V $R'G'B'_0V$
P#5	BV	RG_0BV $R'\ G'_0B'V$
P#6	GBV	$R_0G'BV$ $R'_0GB'V$
P#7	GV	RGBV R'G'B'V
P#8	RGV	RG'BV R'GB'V
P#9	RG	RGB'V R'GB'V

In the hexagonal topology, each node has six neighbors, so, eighteen footprints are possible. Twelve at the edges of the six equilateral triangles where four circles overlap (#P4 to #P9) and six at their centroids (#P1 to #P3), where only three channels are received. Taking into account the XY symmetry (Figure 1b), the R, G and B nodes and their symmetric (R'G'B') must be considered. When the received channels come from outside the hexagon edges (first ring), the nodes are label with *0* (see Figure 1b). When the signal comes only from one LED, the coordinates of the LED are assigned to the device's reference point. If the device receives multiple signals, *i.e.*, if it is in an overlapping region of two or more LEDs, it finds the centroid of the received coordinates and stores it as the reference point.

This is the so called fine-graining of the unit cell.

For data transmission commercially available white RGB-LEDs and a violet (V: 400 nm) LED were used. The output spectrum of the white LED contains three peaks assigned to the colors red (R: 626 nm), green (G: 530 nm) and blue (B: 470 nm), that mixed together provide the white perception to the human eye. Each chip, in the trichromatic LED, can be switched *on* and *off* individually for a desired bit sequence. The luminous intensity is regulated by the driving current for white perception. They exhibit a wide divergence angle (2x60º), since they are also designed for general lighting and allow a wide delivery of the VLC signal around the surrounding area. The driving current of each emitter is controlled independently, suppling the respective coding sequence and frequency [14]. In both topologies, the driving current of the emitters having the same wavelength was always the same.

B. Cellular topologies for large environments

When the rooms are very large, such as in supermarkets or large shopping malls, the positioning technique (four-code assignment for the LEDs), is applied in the whole room.

Thinking about the design, the wall structure could be continued to form the tiles and a complete communication/illumination can be created. For cellular design, a regular shape in needed over the serving area. Squares, equilateral triangles, regular hexagons or a combination of this would be demanding, because the shape makes efficient use of space. They cover the entire area without any gaps decreasing the interference between the same code [24]. Since each cell is projected to use wavelengths only within its boundaries, the same wavelengths can be reused in other close cells without interference.

Like squares, regular hexagons also fit together without any gaps to tile the plane. Ceiling plan for the LED array layout is shown in Figure 1 (LED array = RGBV color spots).

Two topologies were set for the unit cell: the square, (Figure 2a) and the hexagonal (Figure 2b). In the first, the proposed LED arrangement employs four modulated LEDs placed at the corners of a square grid.

The unit cell $C_{i,j}$ is repeated in the horizontal and vertical directions in order to fill all the space. In the second topology (Figure 2b), the hexagonal, the same LED array was used, but in a no-orthogonal system. We select a pair inclined at 120 degrees to be the axes, labelled as X and Y. We have readdressed the nodes, in the oblique Cartesian system. Consequently, in both topologies, each node, $X_{i,j}$, carries its own color, X, (RGBV) as well as its ID position in the network (i,j).

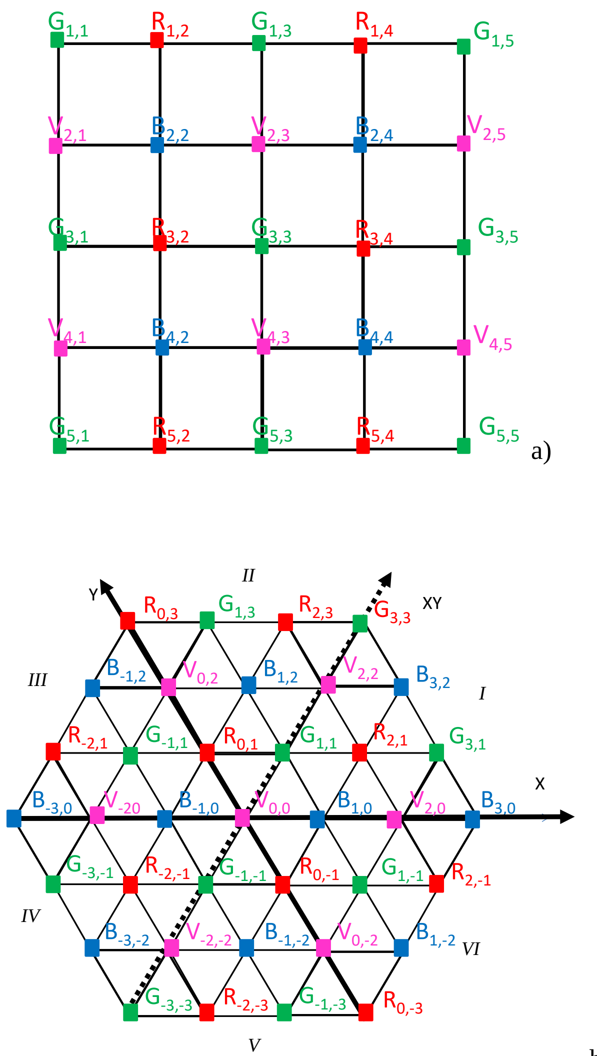

Figure. 2. Illustration of the proposed scenarios (LED array = RGBV color spots): a) Clusters of cells in orthogonal topology (square). b) Clusters of cell in hexagonal topology.

C. The OOK modulation scheme

A dedicated four channel LED driver, with multiple outputs, was developed to modulate the optical signals. The modulation of the emitted light was done through the modulation of the driving electrical current of the semiconductor chips of each LED. The modulator converts the coded message into a modulated driving current signal that actuates the emitters of each violet and tri-chromatic LEDs. A graphical user interface allows the control of the system, which includes the setting of the driving current, bit sequence and frequency of each emitter.

An on-off keying modulation scheme was used. The frame structures are illustrated in Figure 3, for both topologies.

For both, the frame is built based on three separate blocks; the synchronism (Sync), the ID address of the transmitter (ID) and the message to transmit (payload data).

A 32 bit codification was used. The first five bits are used for time synchronization. The same synchronization header [10101], in an ON-OFF pattern, is imposed simultaneously to all the emitters. Each color signal (RGBV) carries its own ID-BIT, so, the next bits give the coordinates of the emitter inside the array ($X_{i,j}$). Cell's IDs are encoded using a binary representation for the decimal number. In the square topology (Figure 3a), six bits are used: the first three for the binary code of the line and the other three for the column. In the hexagonal topology to code the positive and the negative coordinates "sign and magnitude" representation was used, setting bit to *0* is for a positive number, and setting it to *1* is for a negative number.

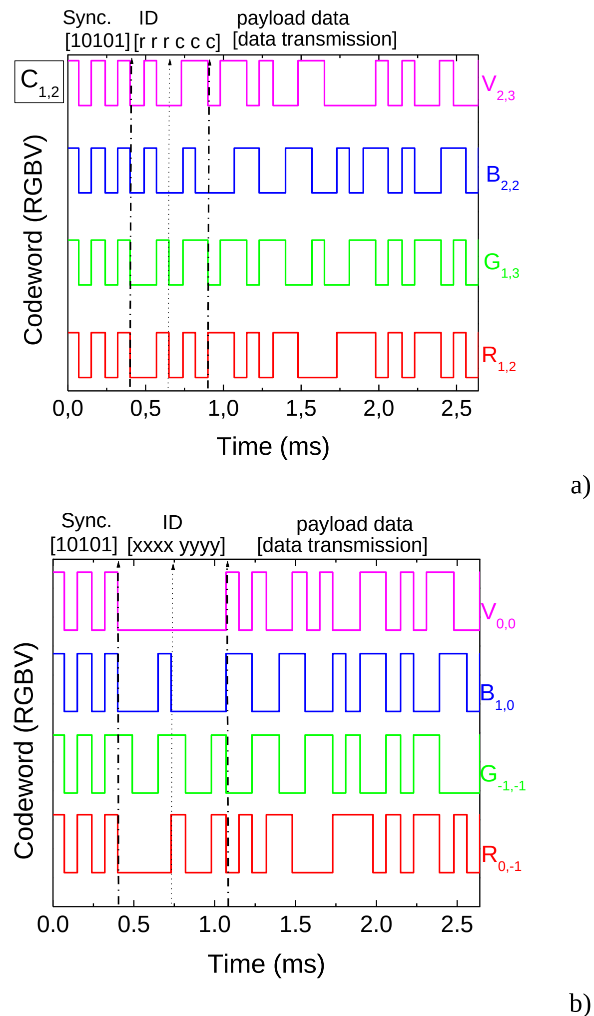

Figure 3. Frame structure. Representation of one original encoded message, in a time slot. a) Square topology; R_{12}; $G_{1,3}$; $B_{2,2}$ and $V_{2,3}$ are the transmitted node packet from the $C_{1,2}$ array in the network.. b) Hexagonal topology; $R_{0,-1}$; $G_{-1,-1}$; $B_{1,0}$ and $V_{0,0}$ are the transmitted node packet of the unit cell in the network.

The remaining bits in the number indicate the absolute value. So, the next eight bits (ID) are assigned, respectively, to the *x* and *y* coordinate (*i*,*j*) of the emitter in the array (Figure 3b). For instance, R_{12} emitter sends a six ID_BIT [001 010] in the square topology while in the hexagonal one the eight ID bits are [0001 0010]. For both, the last bits in the frame are reserved for the message send by the X_{ij} node (payload data). A stop bit is used at the end of each frame.

D. *The VLC receiver*

The VLC receiver is an important component of a VLC system, as its performances are the ones that determine the overall systems performances. The VLC receiver, at the end of the communication link, is responsible to extract the data from the modulated light beam. It transforms the light signal into an electrical signal that is later decoded to extract the transmitted information.

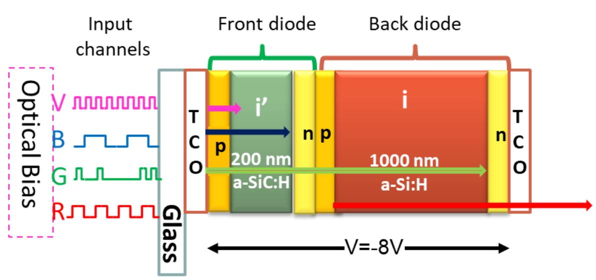

a)

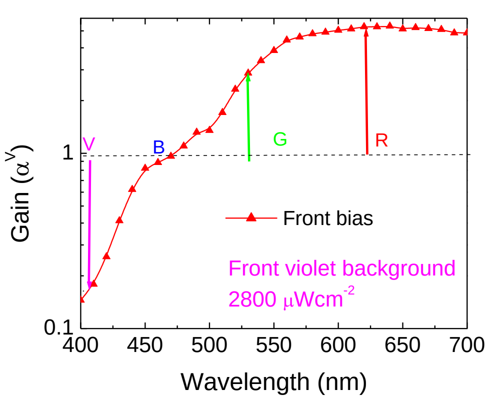

b)

Figure 4. a) Double pi´n/pin configuration and device operation. b) Spectral gain under violet front optical bias (α^V). The arrows point towards the optical gain at the analyzed R, G, B and V input channels.

The VLC receiver is a two terminal, p-i'(a-SiC:H)-n/p-i(a-Si:H)-n photodiode packed in two transparent conductive contacts (TCO).

The deposition conditions, optoelectronic characterization and device optimization are described elsewhere [13]. The configuration and operation is illustrated in Figure 4a. Due to the different absorption coefficient of the intrinsic absorption layers, both front and back diodes act as optical filters confining, respectively, the optical carrier produced by the blue and red light, while the optical carriers generated by the green light are absorbed across both (see arrow in Figure 4a).

The device operates within the visible range using for data transmission the modulated low power light supplied simultaneously by the RGBV LEDs located at the nodes of the array. A mix of R, G, B, and V pulsed communication channels (input channels; transmitted data), each one with a specific bit sequence, impinges on the device and are absorbed accordingly to their wavelengths. The combined optical signal (MUX signal; received data) is analyzed by reading out the generated photocurrent under negative applied voltage and violet background lighting, applied from the front side of the receiver [22, 25]. The optical bias enhances de long wavelength channels (R, G) and quenches the low ones (B,V). In Figure 4b, the spectral gain defined as the ratio between the photocurrent with and without applied optical bias, is displayed. The arrows point towards the gain at the analyzed R, G, B and V input wavelength.

The results show that the device acts as an active filter, under irradiation. It is interesting to notice that, as the wavelength increases, the signal strongly increases. This nonlinearity is the main idea for the decoding of the MUX signal at the receiver.

III. Experimental Results and Discussion

A. *Coding/Decoding techniques*

In Figure 5, the normalized received data due to the mixture of the four R, G, B, and V input channels, i.e., the MUX code signal in a stamp time, are displayed, for the square topology.

In Figure 5a, the bit sequence was chosen to allow all the on/off sixteen (2^4) possible combinations of the four input channels. For three times slots (t_1, t_2, t_3), in Figure 5b, the MUX signal acquired by a receiving positions P#9, P#1, and P#5 (see Table I), is displayed. The decoded packet of transmitted information is presented in the top of both figures. Results from Figure 5a show that the MUX signal presents as much separated levels as the *on/off* possible combinations of the input channels, allowing to decode the transmitted information [26]. All the ordered levels (d_0-d_{15}) are pointed out at the correspondent levels, and are displayed as horizontal dotted lines. In the right hand side of Figure 5a, the match between MUX levels and the 4 bits binary code assigned to each level is shown. Results show that each possible *on/off* state corresponds to a well-defined level. Hence, by assigning each output level to a 4-digit binary code, [X_R, X_G, X_B, X_V], with X=1 if the channel is *on* and X=0 if it is *off*, the signal can be decoded. The MUX signal presented in Figure 5a, is used for calibration purposes. Comparing the calibrated levels with the different generated levels (Figure 5b), in the same frame of time, a simple algorithm [27] is used to decode the multiplex signals.

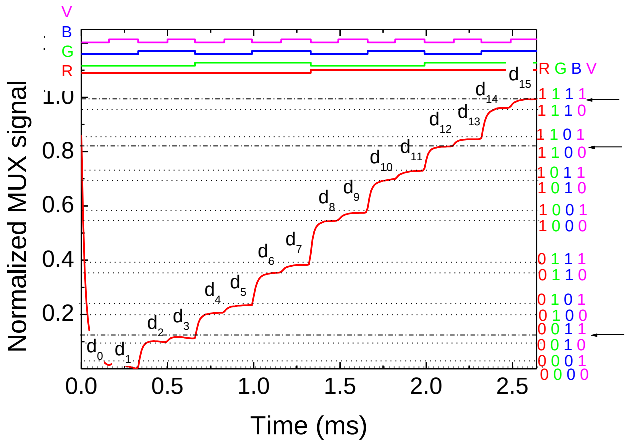

a)

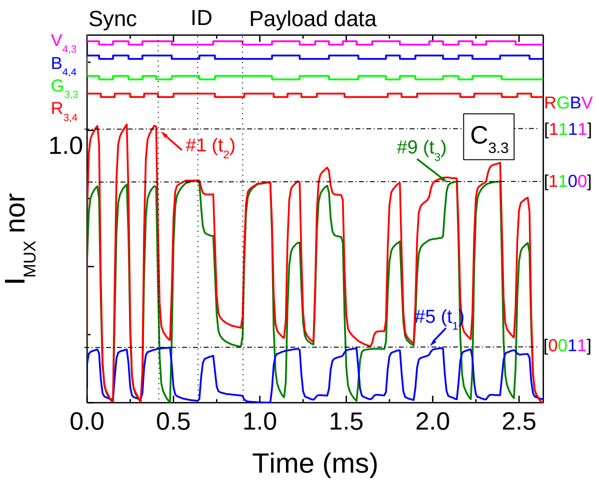

b)

Figure 5. MUX/DEMUX signals under 390 nm front irradiation. On the top the transmitted channels packets [R, G, B, V] are decoded. a) Calibration cell. b) MUX signal in three successive instants (t_1, t_2, t_3).

In Figure 5b, the MUX signal, when the receiver is located in positions P#5, P#1 and P#9 confirms the decoding process. After decoding the MUX signals, the localisation of the receiver is straightforward. Taking into account, the frame structure (Figure 3), the position of the receiver inside the navigation cell and its ID in the network is revealed [28]. The ID position, in the unit cell, comes directly from the synchronism block, where all the received channels are, simultaneously, *on* or *off*. The 4-bit binary code ascribed to the higher level identifies the receiver position in the unit cell (Table I). Those binary codes are displayed in the right hand of the Figure 5b. For instance, the level [1100] corresponds to the level d_{12} where the red and the green channels are simultaneously *on*. The same happens to the other footprints (P#1 and P#9) (see arrows and dash-dot lines in Figure 5a). Each decoded message carries, also, the node address of the transmitter. So, the next block of six bits, in the square topology or eight in the hexagonal one, gives de ID of the received node. In P#5 the location of the transmitters, in the network, are $B_{4,4}$ and $V_{4,3}$ while in P#1 the assigned transmitters are $R_{3,4}$, $G_{3,3,}$ $B_{4,4}$ and $V_{4,3.}$ The last block is reserved for the transmission of the message (payload data). A stop bit (0) is used always at the end of each frame.

B. *LED-aided navigation system*

An interconnection network consists of set of nodes and communication links for the data transmissions. Synchronisation and communication between processing nodes is effectively implemented by message passing. A challenge in LED-based navigation system is the way to improve the data transmission rate while maintaining the capability for accurate navigation. The input of the aided navigation system is the MUX signal, and the output is the system state estimated at each time step (Δt). To compute the point-to-point exposure along a path, we need the data along the path.

As a proof of concept, the suitability of the proposed navigation data bit transition was tested, in the lab. The solution was to move the receiver along a known pattern path. For each transition, two code words are generated, the initial (i) and the final (f). If the receiver stays under the same region, they should be the same, if it moves away they are different. The signal acquisition on the different generated locations was performed and the transition actions were correlated by calculating the ID position codes in the successive instants.

In Figure 6a the simulated path is illustrated and in Figure 6b and Figure 6c MUX/DEMUX signals in six successive instants are displayed. Decoding, when the four channels overlap (P#1), is set on the top of the figures to direct into the packet sent by each node. In the right hand of the figures, the assigned 4-bit binary code is depicted at the successive instants.

Results show that, as the receiver moves between generated point regions, the received information pattern changes. Note that, between two consecutive data sets, there is one navigation data bit transition (a channel is missing or added). We observe that when the receiver initially moves from P#3 to P#1, the green, $G_{1,3}$ and the violet, $V_{2,3}$, channels are added and the 4-bynary bit code changes from [1010] to [1111]. In Figure 6c, the MUX signals acquired in three posterior instants (t_4, t_5, t_6) are displayed. At t_3 the assigned 4-bit [RGBV] code is [0011], changes to [1111] at t_5 and at t_6 it is [1101]. The wavelength of the received emitters, during the transmission, and so the different locations of the receiver inside the cell are assigned as: P#5 (BV), P#1 (RGBV) and P#8 (RGB) (see Table I).

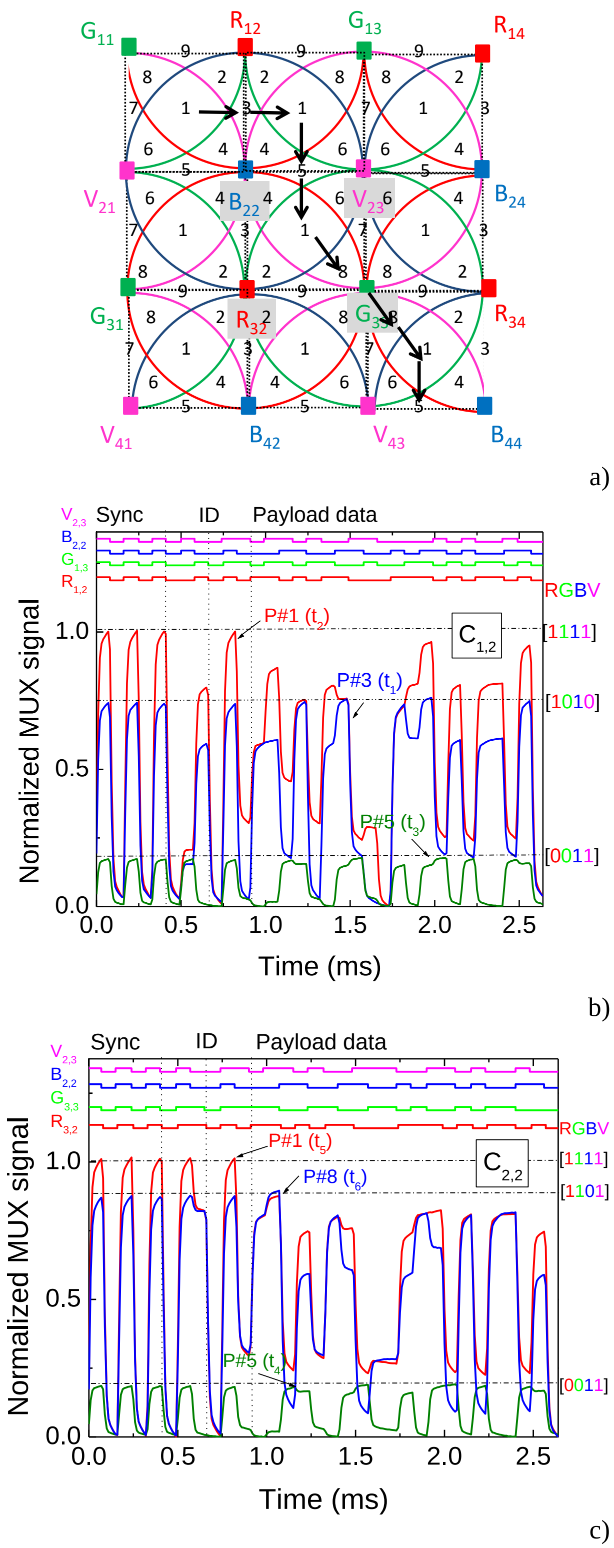

Figure 6 a) Fine-grained indoor localization and navigation in successive instants. Signal acquisition across cell $C_{2,2}$ at t_1, t_2 and t_3, On the top the transmitted channels packets are decoded [R, G, B, V].

Each decoded message carries the node address of the transmitter. The location in the network is decoded through the ID-BIT that carries the address of the node. Looking into the next block of six bits, their position in the network is assigned as: $R_{3,2}$ $G_{3,3}B_{2,2}V_{2,3}$ and linked with $C_{2,2}$ cell. Comparing both P#1 in Figure 6b and Figure 6c, we notice that although the position inside the navigation cell is the same (same level) the location inside the network is different. In Figure 6b the nodes $R_{1,2}$ [001 010], $G_{1,3}$ [001 011], $B_{2,2}$ [010 010] and $V_{2,3}$ [010 011] are recognized and linked respectively, to the cell $C_{1,2}$ while in Figure 6c the assigned nodes are $R_{3,2}$ $G_{3,3}B_{2,2}V_{2,3}$ belong to $C_{2,2}$. At t_4 and t_5 the same two channels are received and linked with P#5, in both figures, the assigned nodes are, $B_{2,2}$ $V_{2,3}$, same position but in different cells (same level in both figures).

Figures 7b and 7c display the MUX/DEMUX signals acquired, in a hexagonal environment (Figure 2b), at six successive instants. The receiver was moved along a known pattern path as described in Figure 7a, the arrows illustrate the simulated path in six successive instants (t_1 to t_6). Fine-grained indoor localization and LED based navigation is illustrated. At the right hand of both figures, the 4-bit binary codes are pointed out at the correspondent levels.

Taking into account Figure 1b and the frame structure (Figure 3b), results show that at t_1 the receiver was located at P#1 [1101]/ $R_{0,-1}$ $G_{-1,-1}$ $V_{0,0}$. At t_2, it arrives to P#7 [1111]/$R_{0,-1}$ $G_{-1,-1}$ $B_{1,0}V_{0,0}$, then, at t_3, moves towards P#2, [1011]/ $R_{0,-1}$ $B_{1,0}V_{0,0}$. At t_4, goes to P#7 [0111]/ $G_{1,1}$ $B_{1,0}V_{0,0}$ and at t_5, arrives to P#6 [1111]/$R_{2,1}$ $G_{1,1}$ $B_{1,0}V_{0,0}$. At t_6, the receiver enters in the second ring, where the 4-binary code [1110] locates the position inside the cell (P#A) and the ID-BIT of the received channels, $R_{2,1}$ $G_{1,1}$ $B_{1,0}$, its position inside the network. The main results show that, for both topologies, the location of a mobile receiver is achieved based on the LED-based navigation system. At the client's end, positioning bits are decided by the received MUX signal (wavelengths and ID address of the received channels). Fine grained localization was achieved by detecting the wavelengths of the received channels in each cell (Table I). Nine sub-regions fill each square cell while in the hexagonal, due to the existing XY symmetry, eighteen possible sub-regions can be designed.

The use of the square, hexagonal or both topologies depends on the layout of the environment. In Figure 8, and for a shopping mall, an example of the mix of both is illustrated. Here, the different areas transmit payload data according to the areas they are located. In concentric layouts, to fill all the space with hexagon, it presents advantages (cosmetics, machines and vegetables areas). Here, the client can move around and walk between the different rings toward the outside region. In an orthogonal layout (hall), the square topology is the best. It allows crossroads and the client can walk easily in the horizontal, vertical or both directions.

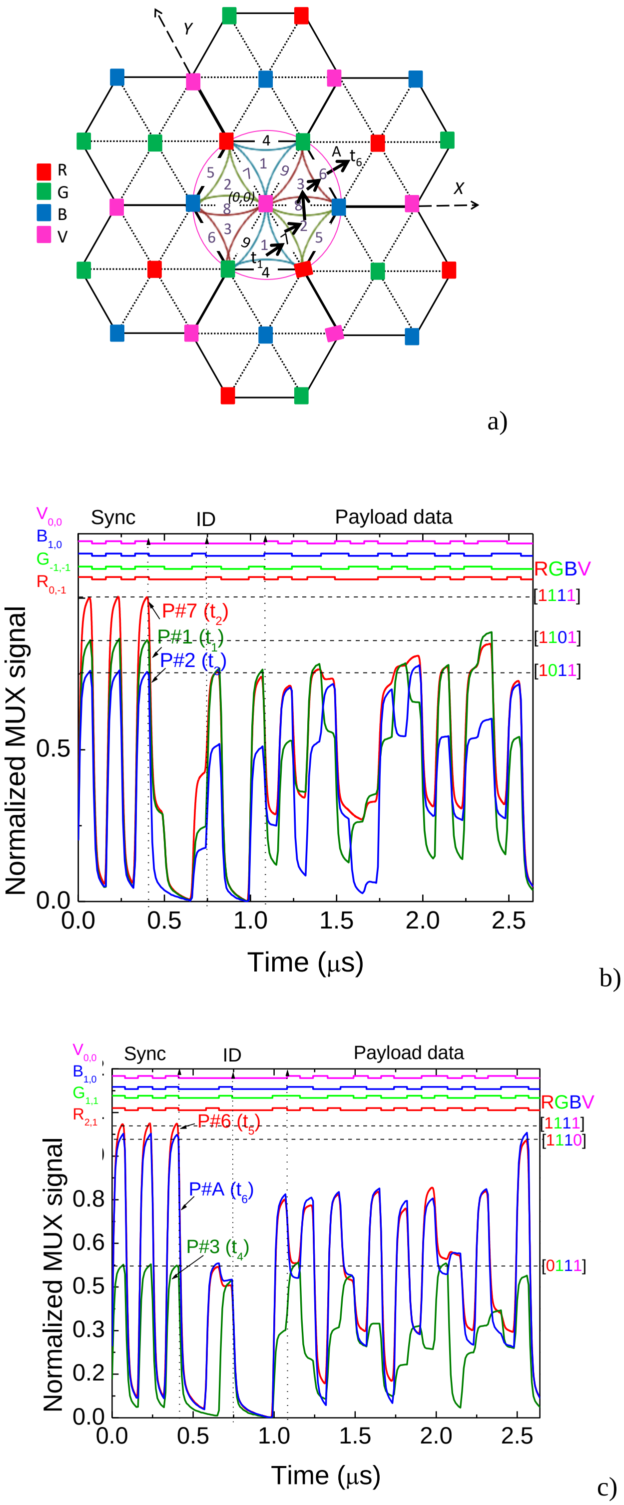

Figure 7 a) Fine-grained indoor localization and navigation, as illustrated by the arrows. b) Signal acquisition at t_1, t_2 and t_3. c) Signal acquisition at t_4, t_5 and t_6 On the top the transmitted channels packets [R, G, B, V] are decoded

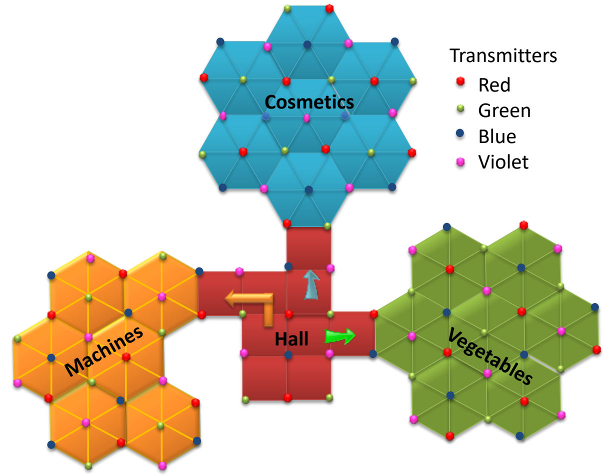

Figure 8 Fusion of hexagonal and square topologies. Example of a ceiling plan. in a shopping mall, with different layout areas. A four-code assignment for the RGBV LEDs is used as positioning technique.

C. *Bidirectional communication*

Bidirectional communication between infrastructure and the mobile receivers can be established. Downlink communication occurs from the ceiling lamps to the mobile receiver.

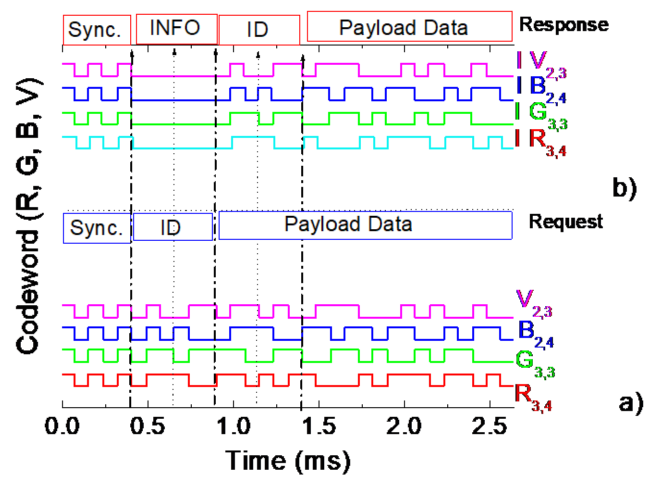

Figure 9 Frame structure representation. a) Codification used to in a request message in P#1. $R_{3,4}$, $G_{3,3}$, $B_{2,4}$ and $V_{2,3}$ are the transmitted node packet, in a time slot. b) Encoded message response of a local controller emitter to the traveler at P#1\ $R_{3,4}$, $G_{3,3}$, $B_{2,4}$ and $V_{2,3}$.

Uplink communication is defined from the receiver to a near indoor billboard linked to the control manager. Each emitter broadcasts a message with its ID and payload data which is received and processed by the receiver. Using a white polychromatic LED as transmitter, the receptor sends to the local controller a message “request” with its location (ID) and adds its queries as payload data (right track, shops, products, etc,). For path coordination, the local controller emitter sends the "response" message with the required information.

In Figure 9a an example of the codification used in a "request" message is illustrated. Thus, $R_{3,4}$, $G_{3,3}$, $B_{2,4}$ and V_{23} are the transmitted node packets, in a time slot, inside the cell in position P#1. In Figure 9b, a "response" message from the controller emitter located at the billboard is displayed. The second block (INFO) in a pattern [000000] means that a response message is being sent by the controller manager. The third block (6 bits) identifies the receiver (ID) for which the message is intended. Here, the controller [000000] responds to a request of a traveller located in position P# 1 ($R_{3,4}$, $G_{3,3}$, $B_{2,4}$ and V_{23}) (see Figure 2a).

In Figure 10, the MUX signal assigned to a "request" and a "response" message are displayed. In the top the decoded information is presented. In the right side, the match between the MUX signal and the 4-binary code is pointed out.

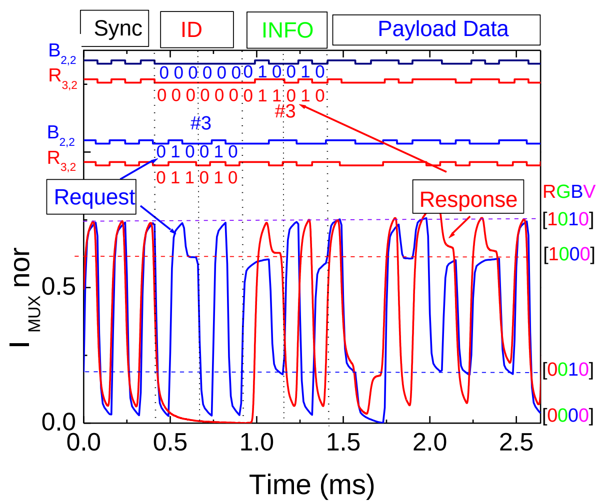

Figure 10. MUX/DEMUX signals assigned to a "request" and a "response" message. On the top the transmitted channels packets [$X_{i,j}$] are decoded.

Here, in a time slot, the traveler, in position #3 ($R_{3,2}$, $B_{2,2}$), sends to the central controller the message "request" in order to add the points of interest (shops or the right track). After that it is advised, through a "response" message, that the request was received, how to reach its destination and how to use location based advertising.

Taking into account the frame structure, results show that the codification of both signals is synchronized (Sync). The request message includes the complete address of the traveler (Sync+ID) and the help need (Payload Data). In the "response" message the block (ID), in a pattern [000000], means that a response message, from the local manager, is being sent. The next block (6 bits) identifies the address (INFO) for which the message is intended and finally in the last block appears the requested information (Payload Data). Here, the emitter controller [000000] responds to a request of a passenger located in position # 3 ($R_{3,2}$, $B_{2,2}$) and sends to him the requested information.

IV. Conclusions and Future Trends

We have proposed a VLC LED-assisted navigation system for large indoor environments. For illumination purposes, data transmission and positioning, white LEDs were used. An a-SiC:H/a-Si:H pin/pin SiC optical MUX/DEMUX mobile receiver decodes the data and based on the synchronism and ID of the joint transmitters it infers its path location. A four-code assignment for the LEDs was proposed. Two cellular networks were tested and compared: the square and the hexagonal. Results show that, in large indoor environments, the use of VLC technology allows different cellular topologies where locations together with data transmission are achieved. The choice of one or both topologies depends mainly on the layout of the environment. Bidirectional communication between the infrastructure and a mobile receiver was also tested.

Minding the benefits of VLC, it is expected that this type of communication will have an important role in positioning applications. Moving towards real implementation, the performances of such systems still need to improve. As a future goal, we plan to finalize the embedded application, for experimenting in several network layouts.

Acknowledgements

This work was sponsored by FCT – Fundação para a Ciência e a Tecnologia, within the Research Unit CTS – Center of Technology and systems, reference UID/EEA/00066/2013
The projects: IPL/2018/II&D_CTS/UNINOVA_ISEL and by: IPL/IDI&CA/2018/LAN4CC/ISEL, are also acknowledge.

Refeeences

[1] Vieira M., Vieira M. A., Louro P., Vieira P., Fantoni A., "Light-Fidelity (Li-Fi) Optical Sensing and Detection in Large Indoor Environments,"The Ninth International Conference on Sensor Device Technologies and Applications, SENSORDEVICES 2018.

[2] Yang, C. and Shao, H. R., "WiFi-based indoor positioning," IEEE Commun. Mag., vol. 53, no. 3, 150–157 (Mar. 2015).

[3] Lin, X. Y., Ho, T. W., Fang, C. C. , Yen, Z. S., Yang, B. J., and Lai, F., "A mobile indoor positioning system based on iBeacon technology," in Proc. Int. Conf. IEEE Eng. Med. Biol. Soc., 4970–4973 (2015).

[4] Huang, C. H., Lee, L. H., Ho, C. C., Wu, L. L., and Lai, Z. H., "Real-time rfid indoor positioning system based on Kalman filter drift removal and heron-bilateration

location estimation," IEEE Trans. Instrum. Meas., vol. 64, no. 3, 728–739, (Mar. 2015).

[5] Hassan, N. U., Naeem, A., Pasha, M. A., Jadoon, T., and Yuen, C., "Indoor positioning using visible led lights: A survey,"ACM Comput. Surv., vol. 48, 1–32 (2015).

[6] Harle, R., "A survey of indoor inertial positioning systems for pedestrians," Commun. Surv. IEEE Commun. Surveys Tuts., vol. 15, no. 3, 1281–1293, (2013).

[7] Sun, Y. X., Liu, M., and Meng. Q. H., "Wifi signal strength-based robot indoor localization," in IEEE International Conference on Information and Automation (2014).

[8] Bahl P. and Padmanabhan V. N., "Radar: an in-building rf-based user location and tracking system," in Proc. of IEEE INFOCOM, (2000).

[9] Liu M., and Siegwart, R., "Dp-fact: Towards topological mapping and scene recognition with color for omnidirectional camera," in Robotics and Automation (ICRA), IEEE International Conference, 3503 –3508 (2012).

[10] Liu, M., Qiu, K., Li, S., Che, F., Wu, L., and Yue, C. P., "Towards indoor localization using visible light communication for consumer electronic devices," in Proceedings of the IEEE/RSJ International Conference on Intelligent Robots and Systems (IROS), Chicago, the USA (2014)

[11] Ozgur E., Dinc, E., Akan, O. B., "Communicate to illuminate: State-of-the-art and research challenges for visible light communications," Physical Communication 17 72–85, (2015).

[12] Armstrong, J., Sekercioglu, Y., Neild, A., "Visible light positioning: a roadmap for international standardization," Communications IEEE, vol. 51, no. 12, pp. 68-73, (2013).

[13] Panta K., Armstrong, J., "Indoor localisation using white LEDs,"Electron. Lett. 48(4), 228–230 (2012).

[14] Komiyama, T., Kobayashi, K., Watanabe, K., Ohkubo, T., and Kurihara, Y., "Study of visible light communication system using RGB LED lights," in Proceedings of SICE Annual Conference, IEEE, 2011, pp. 1926–1928.

[15] Wang, Y., Wang, Y., Chi, N., Yu, J., and Shang, H., "Demonstration of 575-Mb/s downlink and 225-Mb/s uplink bi-directional SCM-WDM visible light communication using RGB LED and phosphor-based LED," Opt. Express 21(1), 1203–1208 (2013).

[16] Tsonev, D., Chun, H., Rajbhandari, S., McKendry, J., Videv, S., Gu, E., Haji, M., Watson, S., Kelly, A., Faulkner, G., Dawson, M., Haas, H., and O'Brien, D., "A 3-Gb/s single-LED OFDM-based wireless VLC link using a Gallium Nitride μLED," IEEE Photon. Technol. Lett. 26(7), 637–640 (2014).

[17] O'Brien, D., Minh, H. L., Zeng, L., Faulkner, G., Lee, K., Jung, D., Oh, Y. and Won E. T., "Indoor visible light communications: challenges and prospects," Proc. SPIE 7091, 709106 (2008).

[18] Schmid, S., Corbellini, G., Mangold, S., and Gross, T. R., "An LED-to-LED Visible Light Communication system with software-based synchronization," in 2012 IEEE Globecom Workshops, 1264–1268 (2012).

[19] Jovicic, A., Li, J., and Richardson, T., "Visible light communication: opportunities, challenges and the path to market," Communications Magazine, IEEE, vol. 51, no. 12, pp. 26–32 (2013).

[20] S T. Komine and M. Nakagawa, "Fundamental analysis for visible-light communication system using led lights," Consumer Electronics, IEEE Transactions on, vol. 50, no. 1, pp. 100–107, (2004).

[21] Monteiro E., and Hranilovic, S., "Constellation design for color-shift keying using interior point methods," in Proc. IEEE Globecom Workshops, Dec., 1224–1228 (2012).

[22] Vieira, M., Louro, P., Fernandes, M., Vieira, M. A., Fantoni A., and Costa, J., "Three Transducers Embedded into One Single SiC Photodetector: LSP Direct Image Sensor, Optical Amplifier and Demux Device" Advances in Photodiodes InTech, Chap.19, 403-425 (2011).

[23] Vieira, M.A., Louro, P., Vieira, M., Fantoni, A., and Steiger-Garção, A., "Light-activated amplification in Si-C tandem devices: A capacitive active filter model" IEEE sensor journal, 12, NO. 6, 1755-1762 (2012).

[24] Vieira M. , Vieira, M. A., Vieira, P., Louro P., "Coupled data transmission and indoor positioning by using transmitting trichromatic white LEDs and a SiC optical MUX/DEMUX mobile receiver," Proc. SPIE. 10231, Optical Sensors 2017, 102310G. (May 16, 2017) doi: 10.1117/12.2265189 (2017).

[25] Vieira, M. A., Vieira, M., Silva, V., Louro, P., Costa, J., "Optical signal processing for data error detection and correction using a-SiCH technology" Phys. Status Solidi C 12, No. 12, 1393–1400 (2015).

[26] Vieira, M. A., Vieira, M., Silva, V., Louro, P. and Barata, M., "Optoelectronic logic functions using optical bias controlled SiC multilayer devices". MRS Proceedings, 1536, 91-96 (2013).

[27] Vieira, M. A., Vieira, M., Costa, J., Louro, P., Fernandes, M., Fantoni, A., "Double pin Photodiodes with two Optical Gate Connections for Light Triggering: A capacitive two-phototransistor model," in Sensors & Transducers Journal Vol. 10, Special Issue, February 2011, 96-120 (2011).

[28] Vieira, M. A., Vieira, M., Louro, P.; Silva, V., Vieira, P., "Optical signal processing for indoor positioning using a-SiCH technology," Opt. Eng. 55 (10), 107105 (2016), doi: 10.1117/1.OE.55.10.107105 (2016).